Rom J Morphol Embryol 2022, 63(2):439–447 ISSN (print) 1220–0522, ISSN (online) 2066–8279 doi: 10.47162/RJME.63.2.15

ORIGINAL PAPER

RJME Romanian Journal of Morphology & Embryology http://www.rjme.ro/

Treatment of skin defects with PRP enriched with hyaluronic acid – histological aspects in rat model

ELENA-ALEXANDRA MARINESCU[1)], OLIVIU NICA[1)], ANCA COJOCARU[1)], ILONA MIHAELA LILIAC[2)], ANA-MARIA CIUREA[3)], MARIUS EUGEN CIUREA[1)]

[1)]*Department of Plastic Surgery, University of Medicine and Pharmacy of Craiova, Romania*

[2)]*PhD Student, Department of Histology, University of Medicine and Pharmacy of Craiova, Romania*

[3)]*Department of Oncology, University of Medicine and Pharmacy of Craiova, Romania*

Abstract

Tissue healing is a complex, dynamic process, characterized by the replacement of devitalized and absent cell and tissue structures. This can be obtained by different methods, these being found in the "reconstructive scale", which although it is very rich does not offer a universally valid solution for closing skin wounds. In plastic surgery, platelet-rich plasma (PRP) has proven effective in the treatment of skin graft donor areas, burn wounds, skin grafts, tendons, or varicose ulcers. Also, hyaluronic acid (HA) has found its utility in different areas of medicine, other than the esthetics field, with satisfactory results after its use in various lesions. The aim of our study was to find a method of healing wounds with skin defect that shortens the time of complete epithelialization compared to native healing, which is accessible to any patient both by its simplicity and by the lowest possible costs. So, we decided to test a preparation consisting of PRP and granular HA in this type of wounds on a group of 30 Wistar rats. Corroborating the macroscopic data with the microscopic ones, an important similarity can be observed between the healing of the adjuvant-treated lesion at 14 days postoperatively and the healing of the lesion left to natural healing at 21 days, thus shortening the healing period by seven days.

Keywords: healing, PRP, hyaluronic acid, skin defect, granular tissue.

Introduction

The skin is the largest organ of both humans and animals, and it is an indispensable structure for the body's homeostasis. The skin functions as a barrier to protect the human body from harmful agents of the external environment, such as microorganisms (bacteria, viruses, fungi), radiation, and chemical and physical agents [1, 2]. Furthermore, the skin serves essential roles for the body, such as maintaining the body's fluids and temperature in balance, synthesizing vitamin D, transmitting, and detecting environmental changes, regulating the immune response, and so on [3, 4]. The integrity of its structure is an essential condition for the performance of the body's physiological functions. Being an organ with a very large surface area and directly exposed to the external environment, the skin is susceptible to burns, various wounds, infections, inflammations, accidents, and skin damage caused by the action of physical or chemical factors, or following surgical interventions, neoplastic injuries, etc. [2, 5, 6].

Skin disease diagnosis and treatment have advanced significantly over the past few decades due to the contributions of doctors and researchers. So, the development and use of a wide range of medications and dressings, skin grafts, and certain biological agents have greatly expanded the ways that acute and chronic skin lesions can be treated [7–10].

In the past two decades, platelet-rich plasma (PRP) has been utilized experimentally and therapeutically to treat a variety of skin conditions. PRP appears to supply large amounts of growth factors and cytokines, which promote angiogenesis and connective cell proliferation [11–13].

Aim

In the present study, we aimed to evaluate the effects of PRP combined with hyaluronic acid (HA) in the healing of skin lesions using experimental optical microscopy studies.

Materials and Methods

The experiment aims to find a method to facilitate the healing of wounds with a skin defect and to develop a protocol as reliable and safe as possible for the patient.

The experiment was carried out in the Animal Facility of the University of Medicine and Pharmacy of Craiova, Romania, with the consent of the Ethics Committee and it complied with all the rules regarding the protection of animals. The biological samples collected postoperatively were processed in the Research Center for Microscopic Morphology and Immunology of the University of Medicine and Pharmacy of Craiova.

In this experiment, we used 30 Wistar rats, male and female, aged between three and six months and weighing between 350 and 450 g, which were randomly divided into three groups of 10 subjects each. The batches were slaughtered at predetermined time intervals to collect

biological samples, thus batch 1 at seven days postoperatively, batch 2 at 14 days postoperatively, and the third batch at 21 days postoperatively.

Anesthesia protocol

The anesthesia used in this experiment was general anesthesia. Its induction was achieved by subcutaneous injection of Ketamine and Xylazine, in a dose of 90 mg/ 10 mg per kg, being performed by the staff of the Animal Facility of the University of Medicine and Pharmacy of Craiova. The installation of anesthesia was verified by a pinch test at the level of the caudal limbs.

The surgical protocol

The first stage of the surgical protocol consisted in collecting venous blood from the jugular vein. This was done by positioning the rat in supine position, and after performing the scrubbing with 10% Betadine antiseptic solution, a linear incision of approximately 2 cm was made on the midline of the ventral chest wall. The jugular vein was identified on the left side, approximately 1 cm from the midline. A 26G peripheral catheter was used to collect venous blood, with the help of which 4 mL of venous blood were extracted. The collected volume being replaced by 4 mL of sterile saline. The collection of venous blood was carried out in a syringe in which we previously added 0.4 mL of 3.8% Sodium Citrate. After removal of the peripheral catheter, hemostasis was achieved by compression and suturing of the wound at the level of the ventral chest wall.

The second stage of the surgical protocol was represented by the execution of skin defects for the experiment. Thus, after placing the rat in the ventral decubitus, the hair was removed from the level of the posterior chest wall and the preoperative drawing was made, which consisted of marking two circular areas of 1 cm in diameter, with a distance of 2 cm between them. The skin was excised up to the level of the fascia, after performing the scrubbing with 10% Betadine solution.

Preparation of PRP enriched with HA

As a result of collection of venous blood, a quantity of approximately 4.5 mL of product was obtained. It was transferred to a 5 mL test tube and after a slight homogenization achieved by circular movements, it was centrifuged at 1500 rpm for 15 minutes. After centrifugation, 2 mL of PRP were extracted, which was activated using Calcium Gluconate of 96 mg/mL, in a ratio of 1:10.

The PRP thus obtained was combined with granular HA, with a molecular mass between 10 and 25 kDa. For each mL of PRP, 25 mg of granular HA was added. This was progressively incorporated into the PRP by circular motions until a homogeneous, adherent gel-like mass was obtained.

The product thus obtained was applied to the wound on the right side of the rat in a thick layer so as to cover the entire lesion, and the wound on the left side was allowed to heal natively.

After applying the PRP enriched with granular HA over the wounds, a hydrofilm dressing was applied.

The two-step surgical protocol was performed on two subjects per batch, with blood drawn from one individual providing enough PRP to treat five subjects per batch. For the remaining eight individuals in the group, only the second step of the surgical protocol was performed.

During the experiment, the macroscopic wounds were observed at seven, 14 and 21 days, respectively.

At the end of each predetermined period, namely seven, 14 and 21 days postoperatively, the laboratory animals were sacrificed, and samples were collected for microscopic and immunohistochemical (IHC) examination. Excision of the parts sent to the laboratory was performed up to the level of the fascia.

Histopathology and image analysis

The harvested tissues were routinely fixed in 10% neutral buffered formalin and embedded in paraffin blocks. Sectioning of paraffin blocks was performed with a rotary microtome (Thermo Fisher Scientific, Waltham, MA, USA) and serial sections of 4 μm thickness each were obtained. Sectioning was followed by deparaffinization and rehydration by passing through successive xylene baths, decreasing concentrations of ethanol solutions, till distilled water. After this process, Hematoxylin staining, washing and rapid differentiation in alcohol–hydrochloric acid and then Eosin staining was performed. After staining, the slides were dehydrated in increasing concentrations of ethanol solutions, clarified in xylene, and mounted. Hematoxylin–Eosin (HE)-stained slides were studied under a light microscope (Nikon 55I), and random images were captured using a 40× objective.

Trichrome staining of slides was performed using the Masson–Goldner trichrome method. Slides were deparaffinized and washed in distilled water. Then six drops each of Hematoxylin–Iron Weigert type A and B were applied for 10 minutes. After draining the slides, 10 drops of stable Picric Acid solution were added without washing for four minutes. A quick wash in distilled water was performed, after which 10 drops of Ponceau/Acid Fuchsin (Masson) were added for four minutes. After washing in distilled water, 10 drops of Phosphomolybdic Acid solution were added for 10 minutes. After removing the reagent, 10 drops of Goldner's light green solution were added by draining without washing and allowed to act for five minutes. Subsequently, the slides were washed in distilled water and passed through successive ethanol baths of increasing concentrations, resting for one minute in the absolute ethanol bath, followed by clearing in xylene and mounting the slides. The slides were studied in light microscopy, and images were captured using a 40× objective.

For immunohistochemistry, the slides were first deparaffinized and rehydrated in graded alcohols, then antigen retrieval was performed by microwaving in Citrate pH 6 buffer. Inactivation of endogenous peroxidase was achieved using 3% Hydrogen Peroxide for 30 minutes, followed by immersion in skim milk for an additional 30 minutes to block nonspecific endogenous sites. Next, the primary antibodies were added on the slides and incubated at 4°C for 18 hours [alpha-smooth muscle actin (α-SMA), mouse, 1:100, Dako (Dako, Glostrup, Denmark); cluster of differentiation 68 (CD68), mouse, 1:50, Abcam (Abcam PLC, Cambridge, UK)]. Next day, after washing, an anti-mouse peroxidase-labeled secondary antibody was added on the slides for two hours (Vector Laboratories, Burlingame,

CA, USA). The slides were treated with 3,3'-Diaminobenzidine (DAB) to visualize the signal, and the nuclei were labeled using a Hematoxylin solution. The slides were dehydrated through successive ethanol solutions, clarified in xylene and coverslip with Canada balsam. Random images were captured using a 10× objective, on the Nikon Eclipse E200 microscope, and archived for further analysis. For all histology and immunohistochemistry images to be quantified, the areas of interest were selected by manually defining a red, green, blue (RGB) color profile, based on the automated thresholding tool in Image-Pro Plus AMS image analysis package (Media Cybernetics, Bethesda, USA), after which the same profile was kept constant for all images in the same set, and areas and integrated optical densities (IODs) were measured and collected in Excel sheets. Data were averaged per animal and per animal group (treatment and control, at seven, 14 and 21 days), and then *t*-test was performed to evaluate the differences between control-treated pairs. Statistical significance was established at $p<0.05$. To process the data obtained from the experiment, we used Microsoft Excel and GraphPad Prism 9.

Results

Histology and histopathology

Macroscopically, after the first seven days we did not notice a major change between the control and test lesions, both cases not showing re-epithelization of the wound. On the 14th day, the macroscopic differences were visible between the two wounds, so that at the level of the control, the wound was healed in a proportion of 40–60%, and at the level of the test in a much higher proportion, of 80–90%. On day 21, we noticed at the control level a macroscopic appearance similar to the appearance of the test at 14th day, while the test was completely healed, with the presence of a good quality elastic scar, including hairs at the level where the defect was created.

Microscopically, there was no epidermis in both lesions at seven days, with either a thinner epidermis or still with freely exposed dermis at 14 days, and with thicker epidermis for both animal groups at 21 days after surgery (Figure 1, A–D). Considerable differences existed at the level of the newly formed epidermis, so at 14 days, at the level of the control the epidermis had an average of 12 µm, and at the level of the test an average thickness of 22 µm ($p<0.001$) (Figure 1E). At 21 days after the lesion, the difference was maintained, with an average thickness of 23 µm for controls, and of 30 µm for the treated group ($p<0.001$) (Figure 1E).

Granulation tissue evolved from early phases with remnant tissue debris, inflammatory cells, thin-walled capillaries and extravasated red blood cells interspersed with a fine collagen network, gaining more collagen fibers, and loosing inflammatory cells and capillaries, as the wound healed in the 14th and 21st days after the lesion (Figure 1F). At 21 days postoperatively, there was an important increase in granulation tissue in both the control and treated groups. At the level of the treated area, on day 21, there was a significant decrease in granulation tissue in all individuals examined and a significant increase in the epidermis, including the appearance of hair follicles at this level.

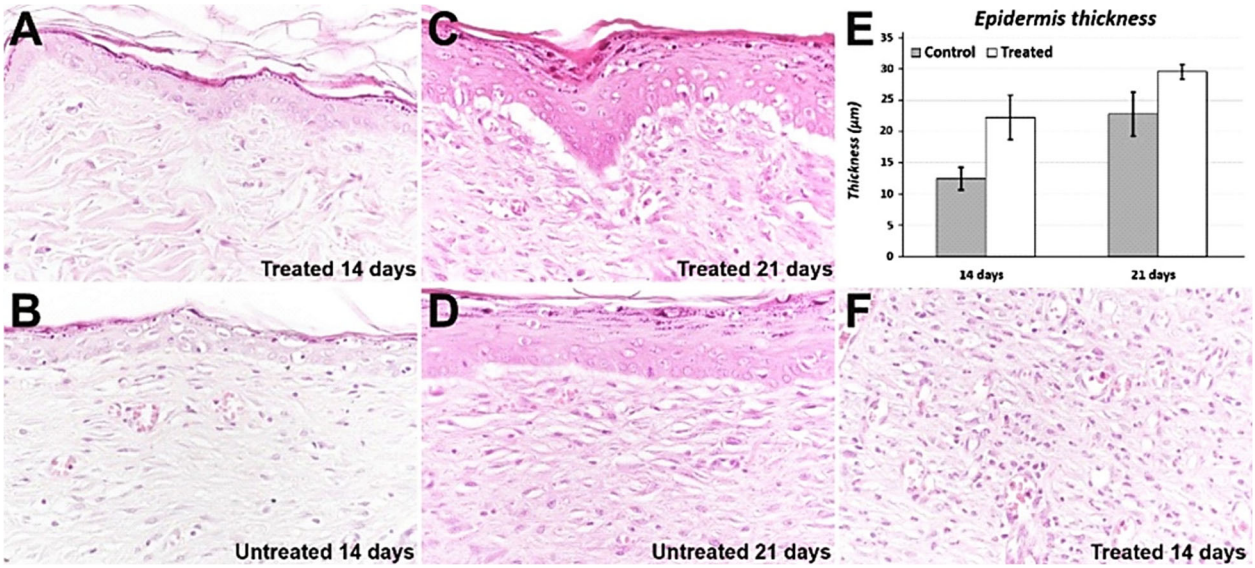

Figure 1 – ***Morphology of the wound repair and re-epithelization process. Apparition of thin layer of epidermis on top of the developing granulation tissue could be first detected at 14 days in both groups (A and B), with full mature epidermis at 21 days (C and D), with a variable degree of adnexal regeneration. Thickness of the epidermis was higher in the treated group compared to the untreated group (E), and granulation tissue matured up towards 14 days (F), exhibiting denser and denser collagen fibers, less blood vessels and inflammatory infiltrate. Hematoxylin–Eosin (HE) staining: (A–D and F) 40×.***

To highlight the collagen fibers density, we used the Masson's trichrome staining, which revealed a better development and organization in the treated lesions in all three groups examined, compared to the untreated lesions, which healed naturally. Granulation tissue could be evaluated again from this point of view, showing only a minimum of signal at seven days, considering that young granulation tissue is a young type of connective tissue rich in ground substance and only with scant collagen fibers, and with progressively thicker bundles of collagen towards 14 and

21 days (Figure 2, A–F). Analysis of the collagen fibers based on the RGB profile of the blue tint of the Masson's collagen technique revealed a progressive increase in staining density (reported as IOD) from the seven days groups to 14- and 21-days groups (Figure 2G), with significantly higher density staining for the treated group compared to controls, at each of the three time points (p<0.001). Interestingly, not only that the difference was maintained, but it was even accentuated for the 21 days group compared to 14 days group and respectively the seven days group. This shows that while both the control and the treated groups started with the same initial pathology, the reparation process developed at different rates, with a more accentuated metabolism in the treated group. We have next assessed the signal area given by the Masson's pigment and a proportional evolution was observed (Figure 2H), paralleling the IOD analysis. Highly significant differences were again obtained for all pairs at each of the three time points, with a difference amplitude increase for the 14 days group and, respectively, for the 21 days group (p<0.001).

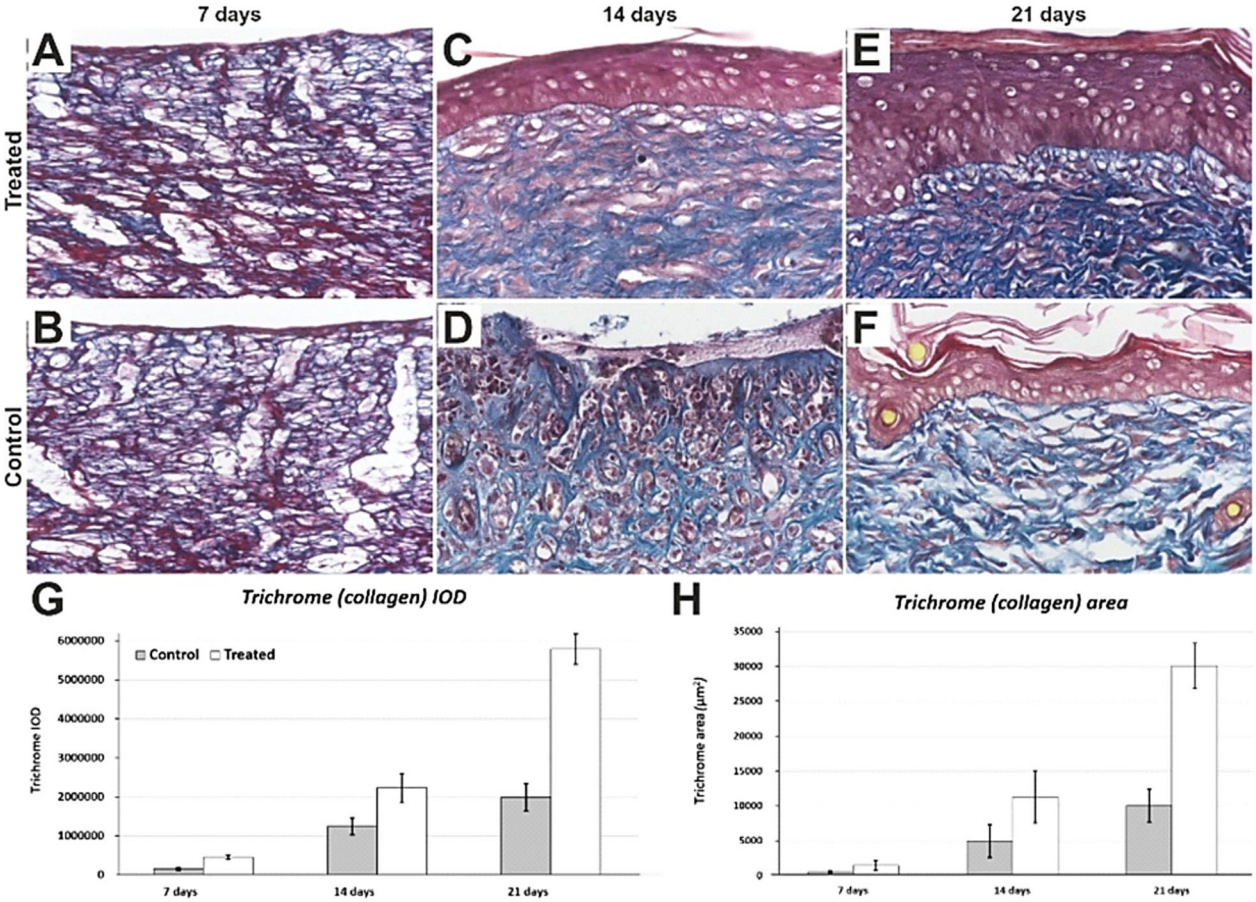

Figure 2 – ***Morphology of the wound repair and stromal density increase. A Masson's trichrome staining best illustrates stromal density variation at the three time points and with the two treatment options (A–F). Both intensity (IOD) and area of the collagen staining revealed almost no fibers at seven days and then an abrupt increase towards the 14- and 21-days' time points (G and H). Masson's trichrome staining: (A–F) 40×. IOD: Integrated optical density.***

In the group sacrificed at seven days, a better expression of collagen was found in the treated areas, with 226% higher values for the area and 265% higher for the IOD, compared to the untreated areas. At 14 days postoperatively, a better representation of collagen is preserved in the lesions where PRP enriched with granular HA was applied compared to untreated areas. The measurements revealed higher values by 103% of the area at the level of the treated areas and by 93% of the IOD, compared to the untreated lesions. For batch 3, sacrificed on day 21, a representation of collagen was observed at the level of the treated area three times higher compared to the values obtained for the areas that healed naturally.

Immunohistochemistry

We have next attempted to extend our morphological evaluation by assessing the presence of the myofibroblasts and monocytes/macrophages in the developing granulation tissue at the three time points.

α-SMA is a protein found in smooth muscle and in the microfilaments of their contractile apparatus and is used to label smooth muscle cells and myofibroblasts. Myofibroblast activity was demonstrated in both control and treated lesions using anti-α-SMA antibody immunostaining, and automated image measurements were performed on dermic areas after manually removing blood vessels, to eliminate smooth muscle cells in the blood vessels walls.

Our analysis revealed that SMA reactivity did not vary much between 7–14 days, with a clear increase for the 21 days group (Figure 3, A–H). Area analysis revealed significant differences between the treated and control groups (p<0.05) for all three time points (Figure 3G). Intensity

of the staining showed again a constant evolution for the 7- and 14-days control group, but this time with an initial high peak of expression at seven days compared to 14 days for the treated group, illustrating a different myofibroblast dynamics even in the initial moments after wound infliction, for the treated group (Figure 3H). Examination of the slides obtained from the pieces harvested seven days postoperatively showed a more intense myofibroblast activity in the treated areas, evidenced by measuring the area and the IOD of the signal for myofibroblasts. Evaluation revealed 123% more signal expression for treated lesions compared to untreated areas, statistical significance at *t*-test being $p<0.05$.

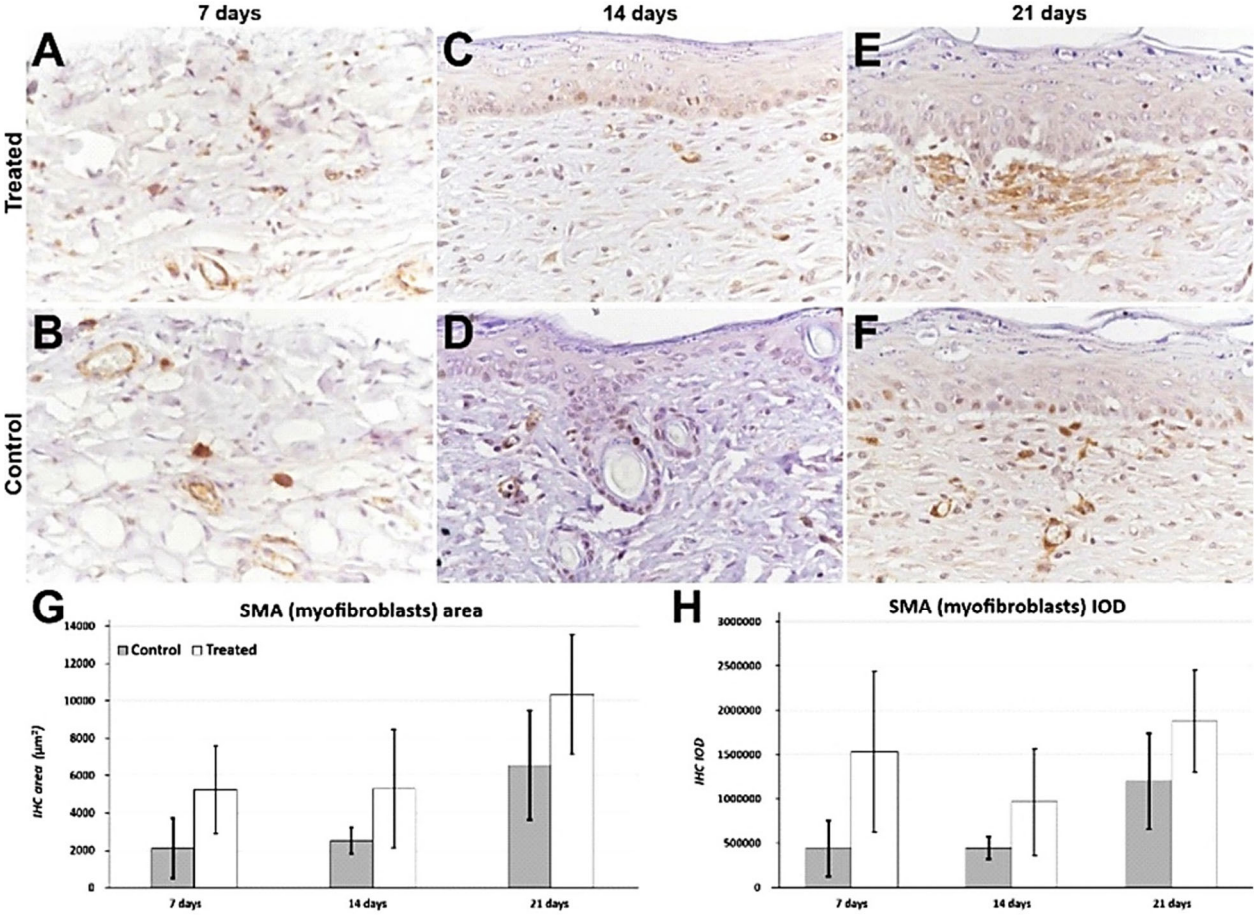

Figure 3 – ***SMA expression at seven, 14 and 21 days after the lesion. Non-vessel associated SMA signal corresponds to myofibroblast activity in the maturing granulation tissue (A–F). Intensity (IOD) and area of the staining revealed robust expression beginning with the 7-day time point, with a plateau for 14 days, and with a drastic increase for the 21-day time point (G and H). Enzymatic SMA immunodetection: (A–F) 40×. Error bars in (G) and (H) represent standard deviation of the means. IHC: Immunohistochemical; IOD: Integrated optical density; SMA: Smooth muscle actin.***

At 14 days postoperatively, the area and IOD of the myofibroblast signal were 54% lower in the areas allowed to heal natively, compared to the treated lesions, the statistical significance in the *t*-test being $p<0.05$. At 21 days post-operatively, the differences between the two working groups were no longer so great in terms of myofibroblast activity, so that the values obtained for area and IOD in untreated wounds were 37% lower compared to the values obtained for wounds treated with PRP enriched with granular HA. Also, close signal values for α-SMA were found between control lesions at 21 days and treated lesions at 14 days, such that the area and IOD values of the 21-day control were 19% higher compared with the test at 14 days.

CD68 is a highly expressed protein within the lysosomal system of macrophages. Anti-CD68 antibody immuno-staining was used to highlight macrophage activity for all three groups in the experiment (Figure 4, A–H).

In the biological samples collected seven days post-operatively, an increased activity of macrophages was found at the level of the test lesions. Area and IOD values for macrophage signal in the control group were 48% lower compared to the test group, with a *t*-test statistical significance of $p<0.05$ (Figure 4G). The difference intensity of the macrophage activity at the level of the treated lesions was maintained at 14 days, so that at the level of the control lesions the signal area represented 48%, and the IOD 45% of the values obtained at the level of the treated areas, the statistical significance in the *t*-test being $p<0.05$.

At 21 days postoperatively, macrophage signal from areas treated with HA-enriched PRP is 60% more intense compared to lesions left to heal naturally, for both area and IOD, with statistical significance at *t*-test of $p<0.05$ (Figure 4H). As for SMA, IOD, however, was able to show a clearer increase in both the absolute values, and in what it regards the treated/untreated ratios, between seven and 14 days.

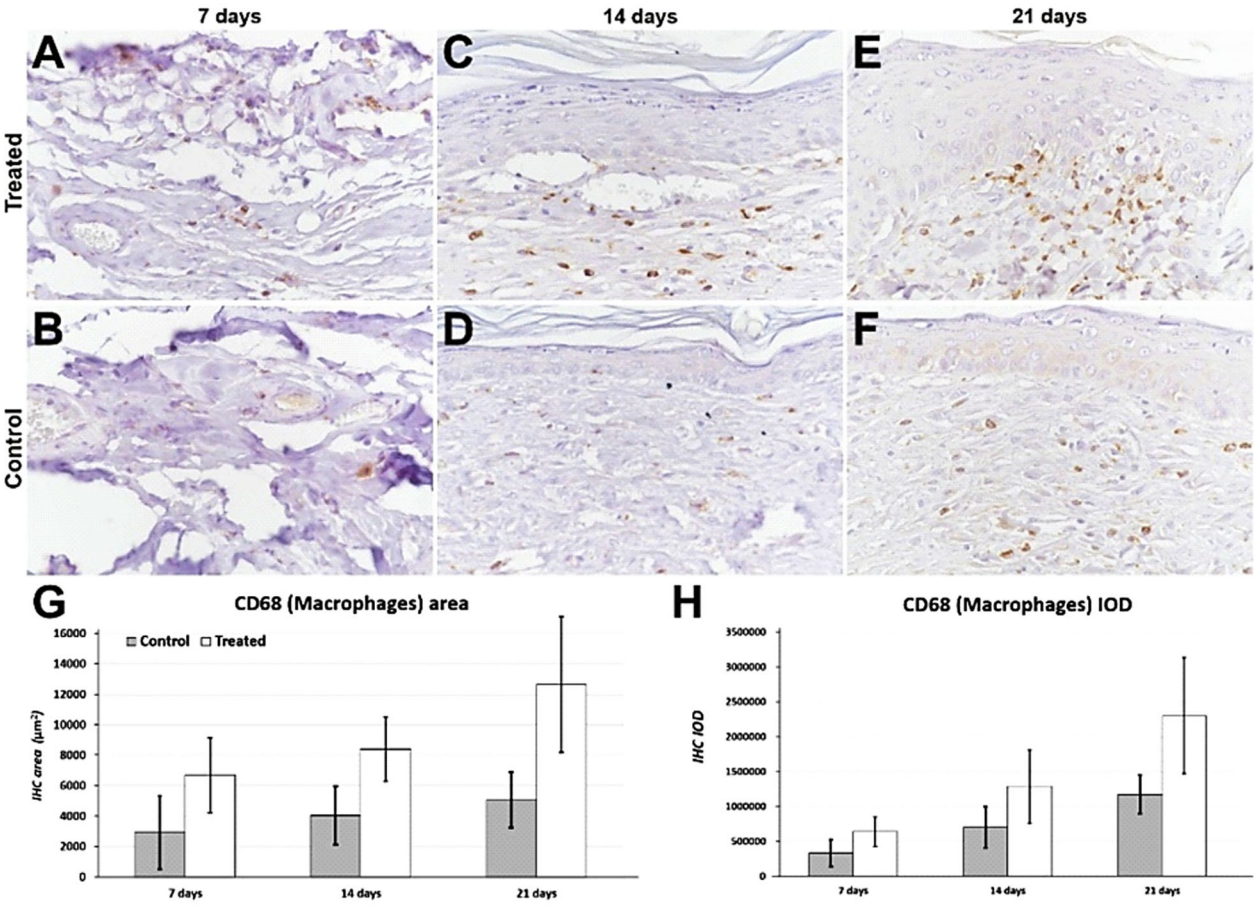

Figure 4 – ***CD68 expression at seven, 14 and 21 days after the lesion. Monocytes/macrophages associated with CD68 expression corresponds to phagocytic/remodeling activity in the maturing granulation tissue (A–F). Intensity (IOD) and area of the staining revealed robust expression beginning with the 7-day time point, with a stepwise increase from 14-day to 21-day time point (G and H). Enzymatic CD68 immunodetection: (A–F) 40×. Error bars in (G) and (H) represent standard deviation of the means. CD68: Cluster of differentiation 68; IHC: Immunohistochemical; IOD: Integrated optical density.***

Discussions

The skin is the largest organ of the human body, with a developed area between 1.5 and 2 m^2 [14], but also the first barrier against external factors, which is why it is permanently exposed to various traumas of greater or lesser intensity. Some of these traumas can have important repercussions, such as wounds with major skin defects, which cannot be closed by direct surgical suturing.

One of the most commonly used methods, but also the handiest for the plastic surgeon is the use of skin grafts, either in partial thickness or in full thickness [15], only that this method, although cheap and easy to approach, is not a 100% safe method when it comes to results and complications. Thus, medical research has focused more on various compounds that could successfully replace the skin graft by replacing the skin prompt or by stimulating a faster and better-quality healing.

Out of the desire to have results as fast, better, but also cheaper, the medical world has sought healing methods that are as reliable as possible and with satisfactory results for both the patient and the doctor.

For the present study, we chose to limit ourselves only to a macroscopic evaluation of the lesions and to a quantitative evaluation of two elements at the microscopic level: the thickness of the granulation tissue and the thickness of the epidermis. Granulation tissue is a very important element in the healing process of a defective wound, both by filling the defect and by preparing a matrix for cell migration and proliferation, but also by forming a protective barrier against microbial agents [16]. Since at the macroscopic examination of the subjects at seven days we did not find major differences between the control lesion and the treated one, we considered useful for the present study the comparison of the lesions on days 14 and 21 postoperatively.

Starting with the 14th postoperative day, the macroscopic differences were visible between the control lesion and the treated one, so that the control lesion was closed approximately 40–60%, while the defect treated with PRP enriched with HA was cured in proportion of 80–90%. On day 21, the macroscopic appearance of the control was similar to that of the treated area at 14 days. At the level of the lesion where adjuvant was applied, after 21 days postoperatively, macroscopically, a complete cure was observed, with the appearance of hairs included.

Microscopically, quantitatively, at 14 days postoperatively, a much greater proliferation of granulation tissue was observed in the treated area, 45% higher compared to the untreated area. Also, in the area treated with PRP enriched

with granular HA, a thickness of the epidermis by 77% was observed compared to the lesions that followed their natural course of healing.

On day 21 postoperatively, at the level of the control area, we noticed an important development compared to day 14 of both the granulation tissue and the epidermis, by 56%, respectively by 77% for the epidermis. The values from day 21 obtained from the untreated lesion are similar to the values from day 14 from the area where the adjuvant was applied.

At the level of the treated area with PRP enriched with granular HA, a significant decrease of the granulation tissue was observed, by 70% compared to the untreated area at the same time interval, but also a 30% increase of the epidermis, which has a similar thickness with that of the epidermis in healthy rats, 32 μm. We also noticed in the epidermis a uniformity of its thickness and the appearance of hair follicles.

Masson's trichrome staining showed the formation of better quality, better organized collagen in the lesions where the adjuvant was applied in the three groups, but also in a much larger quantity, the differences between the two lesions, control and test, being significant.

Several studies have shown that skin wound healing is the consequence of a complex interaction between resident and migrating blood cells, innate and adaptive immune responses, with multiple intercellular communication pathways, requiring a precise balance between tissue repair mechanisms [17, 18]. During the first 24–48 hours, neutrophils and macrophages accumulate at the site of injury, initiating the inflammatory phase and providing protection against pathogens [19]. Platelets are another type of blood cell that promptly intervenes in the repair of the skin and exhibit a variety of membrane receptors that are instantly triggered. When platelets are activated, they release soluble preformed mediators that control how immune cells are recruited and activated [20]. They are primarily involved in the hemostasis phase of wound healing, but their granules contain over 300 diverse molecules: vascular endothelial growth factor (VEGF), epidermal growth factor (EGF), chemokines, cytokines [interleukin (IL)-1, IL-6, transforming growth factor-beta (TGF-β)], etc. [21, 22].

Following the inflammatory phase, the proliferative phase produces granulation tissue by activating fibroblasts and neo-synthesizing extracellular matrix (ECM) components. It also causes neovascularization by creating a new network of vessels and re-epithelializing the wound. It appears that platelets actively participate in the healing of skin wounds by stimulating the proliferation of fibroblasts and keratinocytes, as well as by secreting collagenases during the remodeling phase of the granulation tissue [23]. PRP is a source of growth factors and, consequently, has mitotic, angiogenic, and chemotactic properties, representing an adjuvant treatment alternative for acute and chronic wounds. Furthermore, the application of PRP has been shown to be effective not only in the repair of soft tissues [24, 25], but also in bone and cartilage reconstruction, tendons [26–29], hair growth, etc. The addition of bioactive excipients, such as HA, appears to accelerate endothelial, epithelial, and epidermal regeneration of PRP [30, 31]. However, PRP is far from being standardized and defining the most effective way of application.

In our study, IHC analysis revealed the activity of myofibroblasts and macrophages. The activity of myofibroblasts was more intense in the level of the treated lesions compared to that in the level of the untreated lesions. The signal detected for myofibroblast activity in the test areas was double compared to the control areas, for all three groups.

Myofibroblasts are fibroblast-derived cells that acquire contractile properties by synthesizing α-SMA and other proteins normally found in smooth muscle cells. Myofibroblasts are transient cells that have a special role in wound healing because their contraction reduces the size of the tissue defect that must be filled by scar tissue [32–35].

An intense activity was observed in the treated lesions for macrophages, so following the evaluation of the measurements it was observed that the treated lesions compared to the untreated ones presented a double macrophage activity for all three groups within the experiment.

Numerous studies have shown that after skin injury, monocytes gather on the wound surface and differentiate into macrophages, which subsequently perform phagocytosis to remove damaged cells and tissues, promote angiogenesis, and skin re-epithelialization. They play a key role in the initiation and resolution of inflammatory responses in both acute and chronic injuries [36–40].

Corroborating the macroscopic data and the data obtained after evaluating the histologically processed slides, we can state that the healing of wounds treated with PRP enriched with granular HA is faster by seven days compared to native healing. In favor of this statement can be added the values obtained following the evaluation of the activity of myofibroblasts, which were similar for the lesions treated at 14 days and those not treated at 21 days. However, the data obtained for the assessment of collagen and macrophage activity for the treated areas at 14 days and untreated areas at 21 days showed significant differences.

There is also the problem of obtaining a sterile product since wounds with a skin defect represent entry gates for different pathogens. Although PRP is a product obtained from the patient's blood, and it is a sterile product, granular HA is not presented in a sterile form, and even if it is considered "clean", uncontaminated, its use on human models raises medical ethical issues. Thus, a method of sterilizing the compound formed by PRP and granular HA must be found that does not cancel its properties and that does not inactivate the active compounds involved in the healing process.

Conclusions

Corroborating both macroscopic and microscopic data, an important similarity can be observed between the healing of the adjuvant-treated lesion at 14 days postoperatively and the healing of the lesion left to natural healing at 21 days, which leads to the conclusion that PRP enriched with granular HA accelerate healing by seven days. However, more in-depth studies and close short-term and long-term follow-up of scars resulting from PRP and granular HA treatment are needed to observe possible side effects over time, as well as to find an effective and affordable product sterilization method before it is used in human trials.

Conflict of interests

None to declare.

References

[1] Biggs LC, Kim CS, Miroshnikova YA, Wickström SA. Mechanical forces in the skin: roles in tissue architecture, stability, and function. J Invest Dermatol, 2020, 140(2):284–290. https://doi.org/10.1016/j.jid.2019.06.137 PMID: 31326398

[2] Lin Y, Chen Z, Liu Y, Wang J, Lv W, Peng R. Recent advances in nano-formulations for skin wound repair applications. Drug Des Devel Ther, 2022, 16:2707–2728. https://doi.org/10.2147/DDDT.S375541 PMID: 35996567 PMCID: PMC9392552

[3] Swaney MH, Kalan LR. Living in your skin: microbes, molecules, and mechanisms. Infect Immun, 2021, 89(4):e00695-20. https://doi.org/10.1128/IAI.00695-20 PMID: 33468585 PMCID: PMC8090955

[4] Lee YI, Choi S, Roh WS, Lee JH, Kim TG. Cellular senescence and inflammaging in the skin microenvironment. Int J Mol Sci, 2021, 22(8):3849. https://doi.org/10.3390/ijms22083849 PMID: 33917737 PMCID: PMC8068194

[5] Branisteanu DE, Cojocaru C, Diaconu R, Porumb EA, Alexa AI, Nicolescu AC, Brihan I, Bogdanici CM, Branisteanu G, Dimitriu A, Zemba M, Anton N, Toader MP, Grechin A, Branisteanu DC. Update on the etiopathogenesis of psoriasis (Review). Exp Ther Med, 2022, 23(3):201. https://doi.org/10.3892/etm.2022.11124 PMID: 35126704 PMCID: PMC8794554

[6] Halip IA, Vâţă D, Statescu L, Salahoru P, Patraşcu AI, Temelie Olinici D, Tarcau B, Popescu IA, Mocanu M, Constantin AM, Crisan M, Brihan I, Nicolescu AC, Gheuca-Solovastru L. Assessment of basal cell carcinoma using dermoscopy and high frequency ultrasound examination. Diagnostics (Basel), 2022, 12(3):735. https://doi.org/10.3390/diagnostics12030735 PMID: 35328289 PMCID: PMC8947530

[7] Qu J, Zhao X, Liang Y, Zhang T, Ma PX, Guo B. Antibacterial adhesive injectable hydrogels with rapid self-healing, extensibility and compressibility as wound dressing for joints skin wound healing. Biomaterials, 2018, 183:185–199. https://doi.org/10.1016/j.biomaterials.2018.08.044 PMID: 30172244

[8] Kim HS, Sun X, Lee JH, Kim HW, Fu X, Leong KW. Advanced drug delivery systems and artificial skin grafts for skin wound healing. Adv Drug Deliv Rev, 2019, 146:209–239. https://doi.org/10.1016/j.addr.2018.12.014 PMID: 30605737

[9] Dai C, Shih S, Khachemoune A. Skin substitutes for acute and chronic wound healing: an updated review. J Dermatolog Treat, 2020, 31(6):639–648. https://doi.org/10.1080/09546634.2018.1530443 PMID: 30265595

[10] Cai XC, Ru Y, Liu L, Sun XY, Zhou YQ, Luo Y, Chen JL, Zhang M, Wang CX, Li B, Li X. Efficacy and safety of biological agents for the treatment of pediatric patients with psoriasis: a Bayesian analysis of six high-quality randomized controlled trials. Front Immunol, 2022, 13:896550. https://doi.org/10.3389/fimmu.2022.896550 PMID: 36081503 PMCID: PMC9446895

[11] Anitua E, Andía I, Sanchez M, Azofra J, del Mar Zalduendo M, de la Fuente M, Nurden P, Nurden AT. Autologous preparations rich in growth factors promote proliferation and induce VEGF and HGF production by human tendon cells in culture. J Orthop Res, 2005, 23(2):281–286. https://doi.org/10.1016/j.orthres.2004.08.015 PMID: 15779147

[12] Schär MO, Diaz-Romero J, Kohl S, Zumstein MA, Nesic D. Platelet-rich concentrates differentially release growth factors and induce cell migration *in vitro*. Clin Orthop Relat Res, 2015, 473(5):1635–1643. https://doi.org/10.1007/s11999-015-4192-2 PMID: 25690170 PMCID: PMC4385378

[13] Bouslimani A, Porto C, Rath CM, Wang M, Guo Y, Gonzalez A, Berg-Lyon D, Ackermann G, Christensen GJM, Nakatsuji T, Dorrestein K, Gallo RL, Bandeira N, Knight R, Alexandrov T, Dorrestein PC. Molecular cartography of the human skin surface in 3D. Proc Natl Acad Sci U S A, 2015, 112(17):E2120–E2129. https://doi.org/10.1073/pnas.1424409112 PMID: 25825778 PMCID: PMC4418856

[14] Kia C, Baldino J, Bell R, Ramji A, Uyeki C, Mazzocca A. Platelet-rich plasma: review of current literature on its use for tendon and ligament pathology. Curr Rev Musculoskelet Med, 2018, 11(4):566–572. https://doi.org/10.1007/s12178-018-9515-y PMID: 30203334 PMCID: PMC6220011

[15] Shimizu R, Kishi K. Skin graft. Plast Surg Int, 2012, 2012:563493. https://doi.org/10.1155/2012/563493 PMID: 22570780 PMCID: PMC3335647

[16] Zhang X, Xu R, Hu X, Luo G, Wu J, He W. A systematic and quantitative method for wound-dressing evaluation. Burns Trauma, 2015, 3:15. https://doi.org/10.1186/s41038-015-0013-9 PMID: 27574661 PMC4963942

[17] Gurtner GC, Werner S, Barrandon Y, Longaker MT. Wound repair and regeneration. Nature, 2008, 453(7193):314–321. https://doi.org/10.1038/nature07039 PMID: 18480812

[18] Strbo N, Yin N, Stojadinovic O. Innate and adaptive immune responses in wound epithelialization. Adv Wound Care (New Rochelle), 2014, 3(7):492–501. https://doi.org/10.1089/wound.2012.0435 PMID: 25032069 PMCID: PMC4086194

[19] Rodrigues M, Kosaric N, Bonham CA, Gurtner GC. Wound healing: a cellular perspective. Physiol Rev, 2019, 99(1):665–706. https://doi.org/10.1152/physrev.00067.2017 PMID: 30475656 PMCID: PMC6442927

[20] Mancuso ME, Santagostino E. Platelets: much more than bricks in a breached wall. Br J Haematol, 2017, 178(2):209–219. https://doi.org/10.1111/bjh.14653 PMID: 28419428

[21] Garraud O, Hamzeh-Cognasse H, Pozzetto B, Cavaillon JM, Cognasse F. Bench-to-bedside review: platelets and active immune functions – new clues for immunopathology? Crit Care, 2013, 17(4):236. https://doi.org/10.1186/cc12716 PMID: 23998653 PMCID: PMC4055978

[22] Assinger A, Schrottmaier WC, Salzmann M, Rayes J. Platelets in sepsis: an update on experimental models and clinical data. Front Immunol, 2019, 10:1687. https://doi.org/10.3389/fimmu.2019.01687 PMID: 31379873 PMCID: PMC6650595

[23] De Angelis B, D'Autilio MFLM, Orlandi F, Pepe G, Garcovich S, Scioli MG, Orlandi A, Cervelli V, Gentile P. Wound healing: *in vitro* and *in vivo* evaluation of a bio-functionalized scaffold based on hyaluronic acid and platelet-rich plasma in chronic ulcers. J Clin Med, 2019, 8(9):1486. https://doi.org/10.3390/jcm8091486 PMID: 31540446 PMCID: PMC6780765

[24] Scopelliti F, Cattani C, Dimartino V, Mirisola C, Cavani A. Platelet derivatives and the immunomodulation of wound healing. Int J Mol Sci, 2022, 23(15):8370. https://doi.org/10.3390/ijms23158370 PMID: 35955503 PMCID: PMC9368989

[25] Raţiu IA, Raţiu CA, Miclăuş V, Boşca AB, Turan Kazancioğlu R, Constantin AM, Bako GC, Şovrea AS. The pioneer use of a modified PRGF-Endoret® technique for wound healing in a hemodialyzed diabetic patient in a terminal stage of renal disease. Rom J Morphol Embryol, 2021, 62(2):465–473. https://doi.org/10.47162/RJME.62.2.12 PMID: 35024734 PMCID: PMC8848278

[26] Gentile P, Bottini DJ, Spallone D, Curcio BC, Cervelli V. Application of platelet-rich plasma in maxillofacial surgery: clinical evaluation. J Craniofac Surg, 2010, 21(3):900–904. https://doi.org/10.1097/SCS.0b013e3181d878e9 PMID: 20485077

[27] Cervelli V, Lucarini L, Spallone D, Palla L, Colicchia GM, Gentile P, De Angelis B. Use of platelet-rich plasma and hyaluronic acid in the loss of substance with bone exposure. Adv Skin Wound Care, 2011, 24(4):176–181. https://doi.org/10.1097/01.ASW.0000396302.05959.d3 PMID: 21422842

[28] Fu Q, Zhou R, Cao J, Chen Y, Zhu J, Zhou Y, Shao J, Xin W, Yuan S. Culture of mesenchymal stem cells derived from the infrapatellar fat pad without enzyme and preliminary study on the repair of articular cartilage defects in rabbits. Front Bioeng Biotechnol, 2022, 10:889306. https://doi.org/10.3389/fbioe.2022.889306 PMID: 36061444 PMCID: PMC9428308

[29] Xu AL, Ortiz-Babilonia C, Gupta A, Rogers D, Aiyer AA, Vulcano E. The statistical fragility of platelet-rich plasma as treatment for chronic noninsertional Achilles tendinopathy: a systematic review and meta-analysis. Foot Ankle Orthop, 2022, 7(3):24730114221119758. https://doi.org/10.1177/24730114221119758 PMID: 36051864 PMCID: PMC9424894

[30] Gentile P, Scioli MG, Bielli A, Orlandi A, Cervelli V. Concise review: the use of adipose-derived stromal vascular fraction cells and platelet rich plasma in regenerative plastic surgery. Stem Cells, 2017, 35(1):117–134. https://doi.org/10.1002/stem.2498 PMID: 27641055

[31] Scioli MG, Bielli A, Gentile P, Cervelli V, Orlandi A. Combined treatment with platelet-rich plasma and insulin favours chondrogenic and osteogenic differentiation of human adipose-derived stem cells in three-dimensional collagen scaffolds. J Tissue Eng Regen Med, 2017, 11(8):2398–2410. https://doi.org/10.1002/term.2139 PMID: 27074878

[32] Hinz B. Formation and function of the myofibroblast during tissue repair. J Invest Dermatol, 2007, 127(3):526–537. https://doi.org/10.1038/sj.jid.5700613 PMID: 17299435

[33] Plikus MV, Wang X, Sinha S, Forte E, Thompson SM, Herzog EL, Driskell RR, Rosenthal N, Biernaskie J, Horsley V. Fibroblasts: origins, definitions, and functions in health and disease. Cell, 2021, 184(15):3852–3872. https://doi.org/10.1016/j.cell.2021.06.024 PMID: 34297930 PMCID: PMC8566693
[34] Soliman H, Theret M, Scott W, Hill L, Underhill TM, Hinz B, Rossi FMV. Multipotent stromal cells: one name, multiple identities. Cell Stem Cell, 2021, 28(10):1690–1707. https://doi.org/10.1016/j.stem.2021.09.001 PMID: 34624231
[35] Yao L, Rathnakar BH, Kwon HR, Sakashita H, Kim JH, Rackley A, Tomasek JJ, Berry WL, Olson LE. Temporal control of PDGFRα regulates the fibroblast-to-myofibroblast transition in wound healing. Cell Rep, 2022, 40(7):111192. https://doi.org/10.1016/j.celrep.2022.111192 PMID: 35977484 PMCID: PMC9423027
[36] Baum CL, Arpey CJ. Normal cutaneous wound healing: clinical correlation with cellular and molecular events. Dermatol Surg, 2005, 31(6):674–686; discussion 686. https://doi.org/10.1111/j.1524-4725.2005.31612 PMID: 15996419
[37] Liliac IM, Popescu EL, Văduva IA, Pirici D, Mogoşanu GD, Streba CT, Busuioc CJ, Bejenaru LE, Bejenaru C, Crăciunoiu N, Dumitru I, Elayan H, Mogoantă L. Nanoparticle-functionalized dressings for the treatment of third-degree skin burns – histopathological and immunohistochemical study. Rom J Morphol Embryol, 2021, 62(1):159–168. https://doi.org/10.47162/RJME.62.1.15 PMID: 34609418 PMCID: PMC8597381
[38] Popa GV, Costache A, Badea O, Cojocaru MO, Mitroi G, Lazăr AC, Olimid DA, Mogoantă L. Histopathological and immunohistochemical study of periodontal changes in chronic smokers. Rom J Morphol Embryol, 2021, 62(1):209–217. https://doi.org/10.47162/RJME.62.1.20 PMID: 34609423 PMCID: PMC8597366
[39] Li M, Hou Q, Zhong L, Zhao Y, Fu X. Macrophage related chronic inflammation in non-healing wounds. Front Immunol, 2021, 12:681710. https://doi.org/10.3389/fimmu.2021.681710 PMID: 34220830 PMCID: PMC8242337
[40] Vu R, Jin S, Sun P, Haensel D, Nguyen QH, Dragan M, Kessenbrock K, Nie Q, Dai X. Wound healing in aged skin exhibits systems-level alterations in cellular composition and cell–cell communication. Cell Rep, 2022, 40(5):111155. https://doi.org/10.1016/j.celrep.2022.111155 PMID: 35926463

Corresponding authors

Ana-Maria Ciurea, Assistant, MD, PhD, Department of Oncology, University of Medicine and Pharmacy of Craiova, 2 Petru Rareş Street, 200349, Craiova, Dolj County, Romania; Phone +40749–885 996, e-mail: amciurea14@gmail.com

Ilona Mihaela Liliac, MD, PhD Student, Department of Histology, University of Medicine and Pharmacy of Craiova, 2 Petru Rareş Street, 200349 Craiova, Romania; Phone +40749–059 100, e-mail: ilona.mihaela.liliac@gmail.com

Received: May 5, 2022

Accepted: September 2, 2022